SUPPORTING INFORMATION

A Z-Scheme Photosensitive MOC/g-C_3N_4 Composite Catalyst for Efficient Visible-Light Driven Half and Overall Water Splitting

Xin-Ao Li[a†], Li-Lin Tan[b†], Xiao-Lin Wang[a], Yang Liu[a], Zi-Zhan Liang[a], Jian-Feng Huang[c,], Li-Min Xiao[d], and Jun-Min Liu[a,*]*

*E-mail: huangjf39@scnu.edu.cn; liujunm@mail.sysu.edu.cn

Table of Contents

Experimental Section

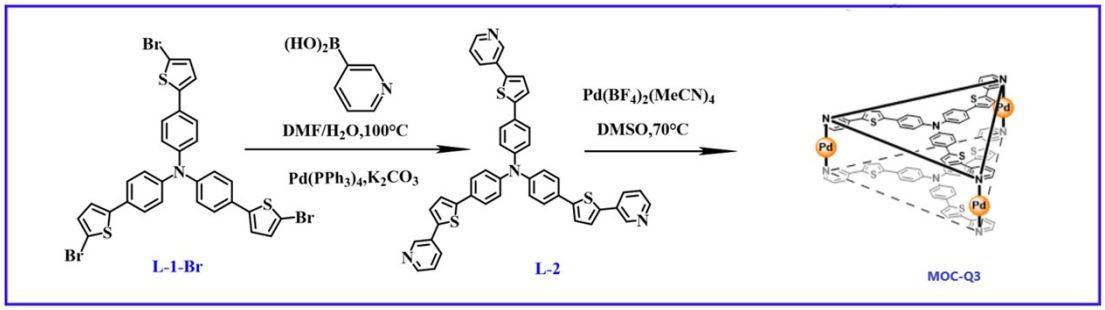

Scheme S1. The synthesis of MOC-Q3.

1. Synthesis of L-1-Br. L-1-Br was prepared according to the previous literature.[1]

2. Synthesis of L-2. L-1-Br (2.30 g, 3.30 mmol), $Pd(PPh_3)_4$ (0.84 g, 0.73 mmol), and 3-pyridinylboronic acid (2.40 g, 19.80 mmol) were mixed in DMF (100 mL) in Schleck bottle, followed by adding K_2CO_3 aqueous solution (8 g, 56.1 mmol, 16 mL). The mixture was heated at 100℃ for overnight under N_2, cooled down, filtered and extracted with dichloromethane. The organic extract was treated with aqueous ammonia and deionized water, dried by anhydrous sodium sulfate and filtrated. Silica-gel column chromatography (PE: EtOAc = 1:4 v/v) was used to purify the crude product and a golden solid L-2 of 1.20 g was obtained. Yield: 50.3%. ^{1}H NMR (400 MHz, DMSO-d_6) δ (ppm): 8.95 (d, J = 2.4 Hz, 1H), 8.51 (d, J = 4.7 Hz, 1H), 8.12-8.05 (m, 1H), 7.74-7.66 (m, 3H), 7.59-7.52 (m, 1H), 7.47 (dd, J = 8.1, 4.8 Hz, 1H), 7.17 (d, J = 8.3 Hz, 2H). ^{13}C NMR (101 MHz, Chloroform-d) δ (ppm): 148.34, 146.67, 146.64, 144.62, 138.91, 132.54, 130.37, 128.95, 126.77, 125.23, 124.51, 123.69, 123.62. ESI-Q-TOF: 723.1705, m/z ($[M+H]^+$). Eelemental analysis ($C_{45}H_{30}N_4S_3$): Theoretical content (C 74.76%, H 4.18%, N 7.75%, S 13.31%); Actual content (C 74.72%, H 4.20%, N 7.80%, S 13.34%).

3. Synthesis of $IrO_2 \cdot xH_2O$ colloid. K_2IrCl_6 (120 mg, 0.25 mmol) and disodium hydrogen citrate (200 mg, 0.85 mmol) were mixed in deionized water (200 mL) in a Schleck bottle to give a reddish

brown solution. The pH of the mixture was adjusted to 7.5 by adding 0.25 M NaOH solution. The solution was stirred and heated at 95℃ for 30 min, during which time it changed from reddish brown to light green. The pH of the solution was then measured again and adjusted to 7.5, followed by stirring for a further 30 min while maintaining the temperature at 95℃. At this stage the solution turned blue. The above steps were repeated until the pH was stabilized at 7.5, resulting in a dark blue solution. Finally, oxygen was introduced into the solution, which was stirred and heated at 95℃ for a further 30 minutes, giving a dark blue colloidal $IrO_2 \cdot xH_2O$.

4. Characterizations. The steady-state and time-resolved photoluminescence (PL) spectra were tested on an Edinburgh FLSP980 fluorescence spectrometer. The cyclic voltammetry (CV) curves were recorded using a CH Instruments CHI760E electrochemical work station. X-ray photoelectron spectroscopy (XPS) were performed in an ultrahigh vacuum chamber (ESCALAB 250Xi) using an XR6 monochromated AlKα X-ray source (hv = 1486.6 eV) with a 900 mm spot size. The Pd contents in the samples were determined using inductively coupled plasma-atomic emission spectrometry (ICP-AES) (SPECTRO CIROS VISION, spectra range: 120-800 nm, and holographic grating: 2924 line/mm).

5. Apparent quantum yield (AQY) measurements for H_2 evolution. 20 mg Catalyst, 9 mL water and 1 mL TEOA were added into a sealed quartz bottle. The mixture was ultrasonic-dispersed and degassed by bubbling with N_2 for 30 min to degass. Then the mixture was stirred and irradiated with a monochromatic LED (Zolix, MLED4-1, λ = 425 nm, 450 nm or 515 nm), which photon flux were determined to be 1083.0 μmol h^{-1}, 1,146.7 μmol h^{-1} and 1,312.3 μmol h^{-1}, respectively. And the H_2 yields were detected by GC. And the AQYs were calculated as the following formula (1):

$$\Phi = \frac{number\ of\ transfered\ electrons}{number\ of\ incident\ photons} \times 100\% = \frac{2 \times n(H_2)}{n(photons)} \times 100\% \quad (1)$$

6. Hydroxyl radical trapping experiment. 20 mg of g-C_3N_4, MOC-Q3 or g-C_3N_4/MOC-Q3 (11 wt%) was dispersed in a sealed 40 mL quartz bottle containing 10 mL aqueous solution containing 5×10^{-4} M terephthalic acid (TA) and 2×10^{-3} M NaOH. Then the mixture was stirred and irradiated under a 300 W Xenon lamp with a 420 nm cut-off filter for 1 h. After irradiation, the mixture was filtered using a membrane filter (aqueous phase), and the filtrate was used for fluorescence measurement.

Table S1. Theoretical and actual MOC contents of g-C_3N_4/MOC-Q3 (7/9/11/13 wt%).

Sample	Measured MOC content / wt%
g-C_3N_4/MOC-Q3 (**7** wt%)	0.18
g-C_3N_4/MOC-Q3 (**9** wt%)	0.23
g-C_3N_4/MOC-Q3 (**11** wt%)	0.27
g-C_3N_4/MOC-Q3 (**13** wt%)	0.33
IrO_2/g-C_3N_4/MOC-Q3	0.26

Table S2. Theoretical and actual IrO_2 contents of IrO_2 (2.04/1.63/1.36 wt%)/g-C_3N_4/MOC-Q3.

Sample	Measured IrO_2 content / wt%
IrO_2 (2.04 wt%)/g-C_3N_4/MOC-Q3	1.76
IrO_2 (1.63 wt%)/g-C_3N_4/MOC-Q3	1.32
IrO_2 (1.36 wt%)/g-C_3N_4/MOC-Q3	1.00

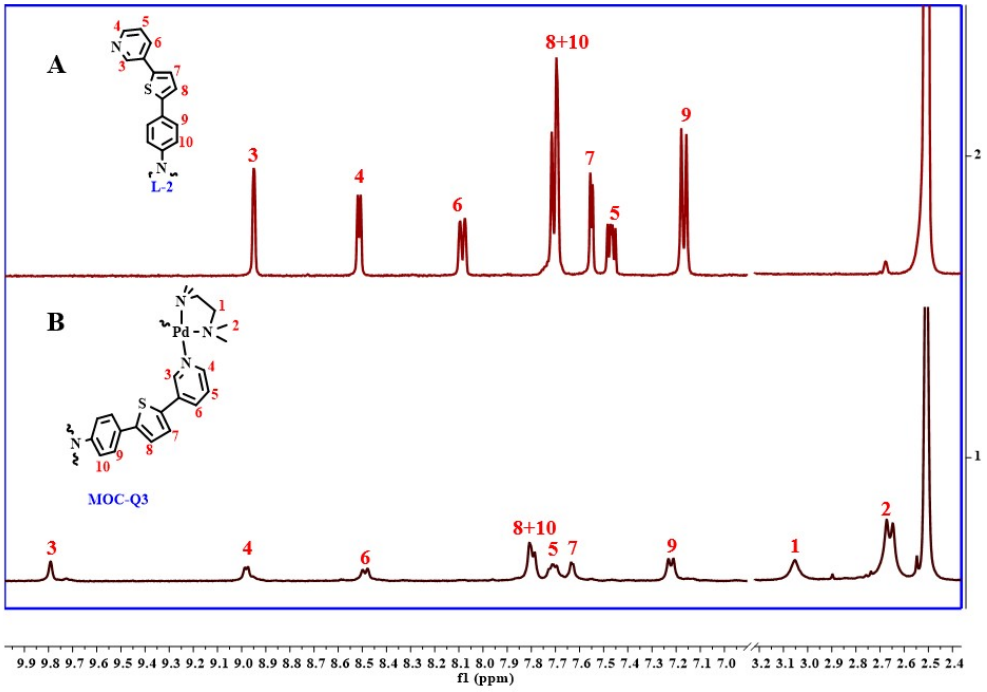

Figure S1. ^{1}H NMR spectra (400 MHz, DMSO-d_6) of A) ligand L-2 and B) MOC-Q3.

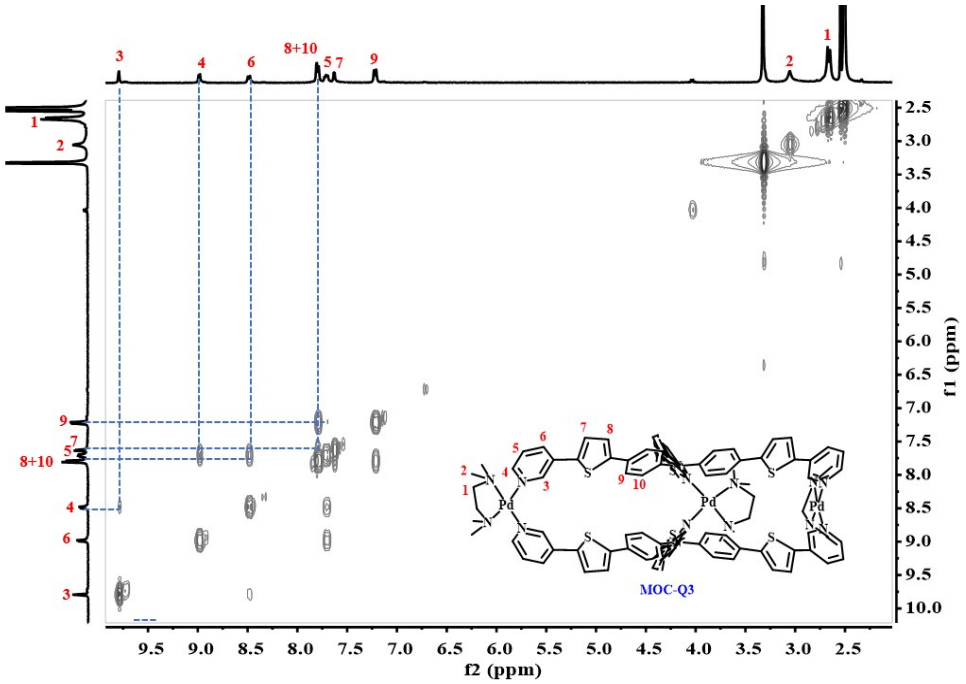

Figure S2. ^{1}H-^{1}H COSY spectrum (400 MHz, DMSO-d_6) of MOC-Q3.

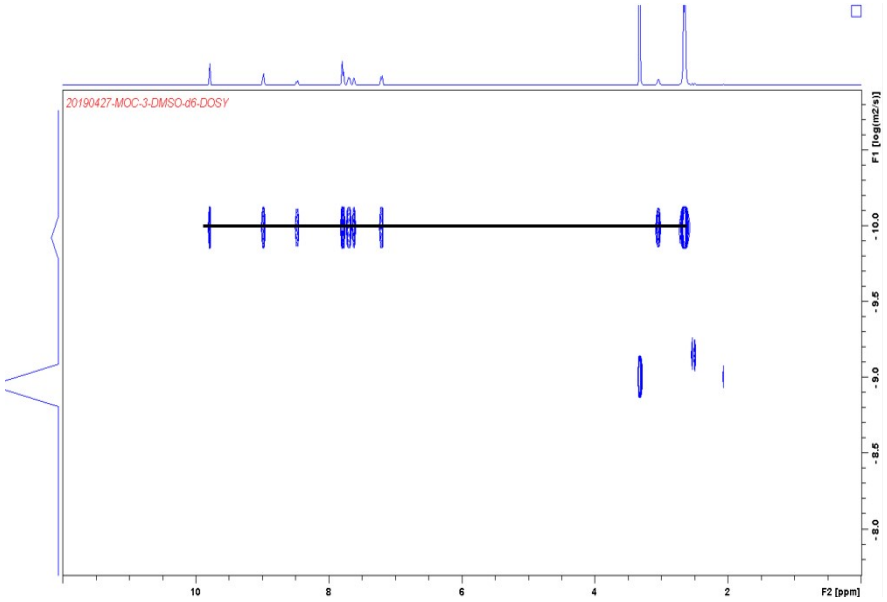

Figure S3. ^{1}H DOSY spectrum (400 MHz, DMSO-d_6) of MOC-Q3.

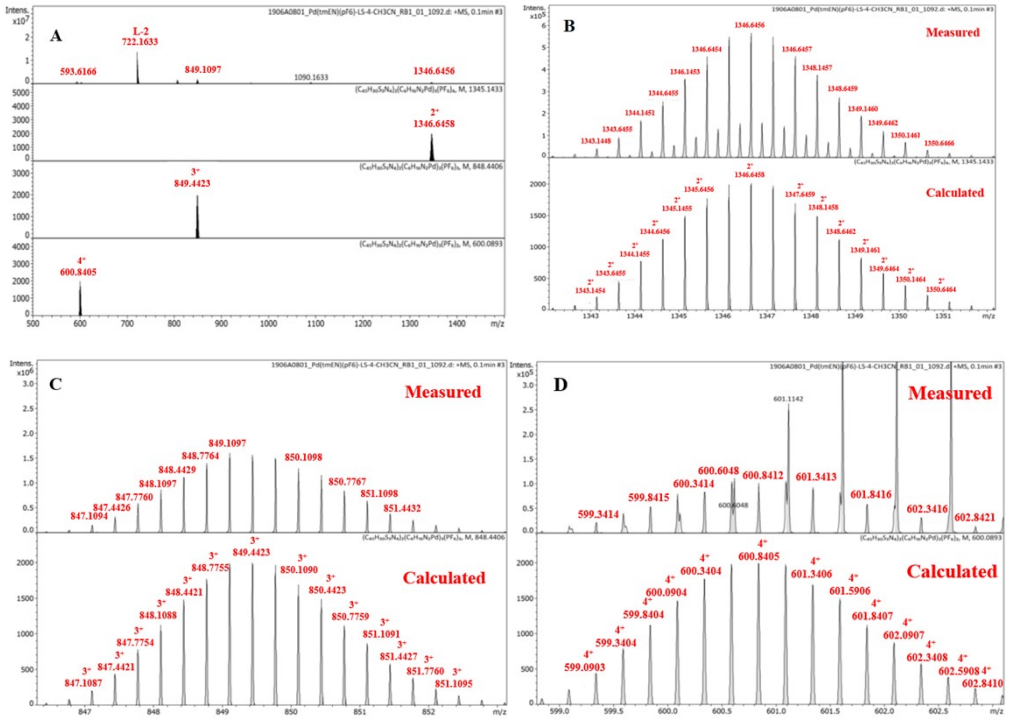

Figure S4. A) Full ESI-MS spectrum, and B-D) ESI-MS spectra of ion peaks for charge states 2^{+}, 3^{+} and 4^{+} of MOC-Q3.

Table S3. The crystal data of MOC-Q3.

MOC-Q3	
Identification code	MOC-Q3
Empirical formula	$C_{105}H_{102}N_{14}Pd_3S_6$
Formula weight	2071.56
Temperature/K	240.00(10)
Crystal system	hexagonal
Space group	$P6_3/m$
a/Å	32.1234(11)
b/Å	32.1234(11)
c/Å	13.3475(5)
α/°	90
β/°	90
γ/°	120
Volume/Å^3	11928.2(7)
Z	2
ρ_{calc}g/cm^3	0.577
μ/mm^{-1}	2.471
F (000)	2128.0
Radiation	Cu Kα (λ = 1.54178)
2Θ range for data collection/°	7.346 to 81.158
Index ranges	$-22 \le h \le 10$, $-22 \le k \le 10$, $-9 \le l \le 10$
Reflections collected	7544
Independent reflections	2564 [R_{in} = 0.0397, R_{sigma} = 0.0491]
Data/restraints/parameters	2564/515/257
Goodness-of-fit on F^2	0.955
Final R indexes [I>=2σ (I)]	R_1 = 0.1348, wR_2 = 0.3490
Final R indexes [all data]	R_1 = 0.1687, wR_2 = 0.3731
Largest diff. peak/hole / e Å^{-3}	0.77/-0.72

Table S4. The bond lengths of MOC-Q3.

MOC-Q3					
Atom	Atom	Length/Å	Atom	Atom	Length/Å
Pd1	N31	2.13(2)	N3	C16	1.489(10)
Pd1	N3	2.13(2)	N1A	C5A	1.39
Pd1	N1A1	2.060(16)	N1A	C1A	1.39
Pd1	N1A	2.060(16)	C5A	C4A	1.39
Pd1	N1	2.075(18)	C4A	C3A	1.39
Pd1	N11	2.075(18)	C4A	C6A	1.464(14)
S003	C9A	1.812(9)	C3A	C2A	1.39
S003	C6A	1.823(9)	C2A	C1A	1.39

S003	C6	1.80(2)	C9A	C8A	1.377(9)
S003	C9	1.78(2)	C8A	C7A	1.437(9)
N2	C132	1.431(17)	C7A	C6A	1.368(9)
N2	C13	1.431(11)	N1	N11	1.73(7)
N2	C133	1.431(16)	N1	C5	1.39
C10	C11	1.39	N1	C1	1.39
C10	C15	1.39	C5	C4	1.39
C10	C9A	1.481(14)	C4	C3	1.39
C10	C9	1.49(2)	C4	C6	1.46(2)
C11	C12	1.39	C3	C2	1.39
C12	C13	1.39	C2	C1	1.39
C13	C14	1.39	C6	C7	1.35(2)
C14	C15	1.39	C7	C8	1.43(2)
N3	C17	1.500(10)	C8	C9	1.38(2)
N3	C18	1.494(10)	C16	C161	1.478(11)

[1]+X, +Y, 3/2-Z; [2]1+Y-X, 1-X, +Z; [3]1-Y, +X-Y, +Z

Table S5. Bond angles of MOC-Q3.

MOC-Q3							
Atom	Atom	Atom	Angle/°	Atom	Atom	Atom	Angle/°
N3	Pd1	N31	78.6(15)	N1A	C5A	C4A	120
N1A1	Pd1	N3	93.3(12)	C5A	C4A	C6A	117.8(17)
N1A	Pd1	N3	171.8(11)	C3A	C4A	C5A	120
N1A	Pd1	N31	93.3(12)	C3A	C4A	C6A	121.9(17)
N1A1	Pd1	N31	171.8(11)	C4A	C3A	C2A	120
N1A1	Pd1	N1A	94.8(17)	C1A	C2A	C3A	120
N1A1	Pd1	N11	22.8(13)	C2A	C1A	N1A	120
N1A	Pd1	N11	72.0(15)	C10	C9A	S003	115.6(11)
N11	Pd1	N3	116.1(13)	C8A	C9A	S003	110.9(5)
N1	Pd1	N3	165.2(13)	C8A	C9A	C10	133.5(12)
N11	Pd1	N1	49(2)	C9A	C8A	C7A	114.1(6)
C9A	S003	C6A	89.7(4)	C6A	C7A	C8A	114.4(6)
C9	S003	C6	92.3(11)	C4A	C6A	S003	122.2(14)
C132	N2	C13	118.8(11)	C7A	C6A	S003	110.8(5)
C133	N2	C13	118.8(11)	C7A	C6A	C4A	126.7(15)
C133	N2	C132	118.8(8)	N11	N1	Pd1	65.4(11)
C11	C10	C15	120	C5	N1	Pd1	118.0(15)
C11	C10	C9A	115.4(13)	C5	N1	N11	107.2(14)
C11	C10	C9	113.3(14)	C5	N1	C1	120
C15	C10	C9A	122.4(14)	C1	N1	Pd1	121.2(15)
C15	C10	C9	126.7(14)	C1	N1	N11	105.0(13)
C10	C11	C12	120	N1	C5	C4	120
C13	C12	C11	120	C5	C4	C3	120

C12	C13	N2	121.6(15)	C5	C4	C6	119(2)
C14	C13	N2	118.4(15)	C3	C4	C6	119.4(19)
C14	C13	C12	120	C2	C3	C4	120
C13	C14	C15	120	C3	C2	C1	120
C14	C15	C10	120	C2	C1	N1	120
C17	N3	Pd1	109.9(15)	C4	C6	S003	116.9(19)
C18	N3	Pd1	107.6(16)	C7	C6	S003	108.8(16)
C18	N3	C17	108.0(9)	C7	C6	C4	133(2)
C16	N3	Pd1	116.6(17)	C6	C7	C8	115(2)
C16	N3	C17	107.1(10)	C9	C8	C7	114(2)
C16	N3	C18	107.4(10)	C10	C9	S003	116.9(16)
C5A	N1A	Pd1	116.5(13)	C8	C9	S003	108.4(16)
C5A	N1A	C1A	120	C8	C9	C10	134(2)
C1A	N1A	Pd1	123.2(13)	C161	C16	N3	114.1(10)

[1]+X, +Y, 3/2-Z; [2]1+Y-X, 1-X, +Z; [3]1-Y, +X-Y, +Z

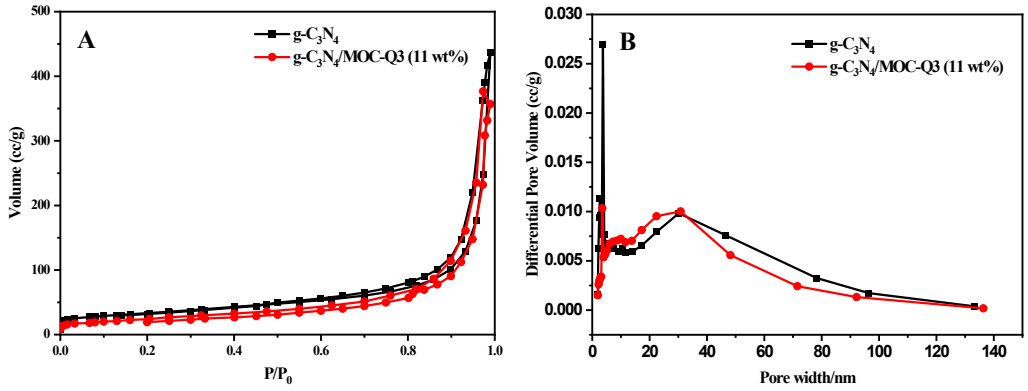

Figure S5. A) N_2 adsorption-desorption isotherms and B) pore size distributions of g-C_3N_4 and g-C_3N_4/MOC-Q3.

Table S6. BET surface areas and pore volumes of g-C_3N_4 and g-C_3N_4/MOC-Q3 (11 wt%).

	g-C_3N_4	g-C_3N_4/MOC-Q3 (11 wt%)
BET surface area / $m^2\ g^{-1}$	115.7	81.5
Total pore volume / $cm^3\ g^{-1}$	0.68	0.58
Microporous pore volume / $cm^3\ g^{-1}$	0.009	——
Mesoporous pore volume / $cm^3\ g^{-1}$	0.68	0.58

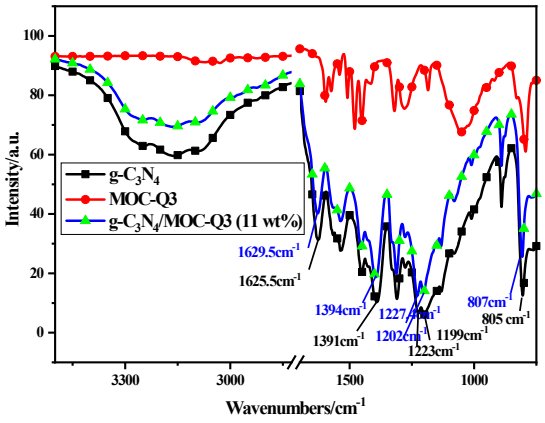

Figure S6. FT-IR spectra of MOC-Q3, g-C_3N_4, and g-C_3N_4/MOC-Q3 (11wt%).

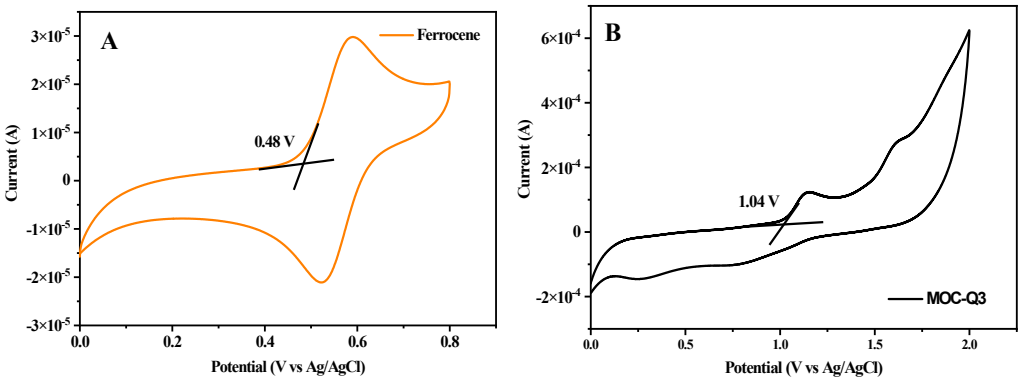

Figure S7. CV curves of A) Ferrocene and B) MOC-Q3 (0.2 mM) in CH_3CN. Room temperature, weep rates 50 mV s^{-1}, Ag/AgCl as reference electrode, graphite rod as counter electrode, platinum wire as working electrode, and 0.1 M tetrabutylammonium hexafluorophosphate ($TBAPF_6$) as support electrolyte.

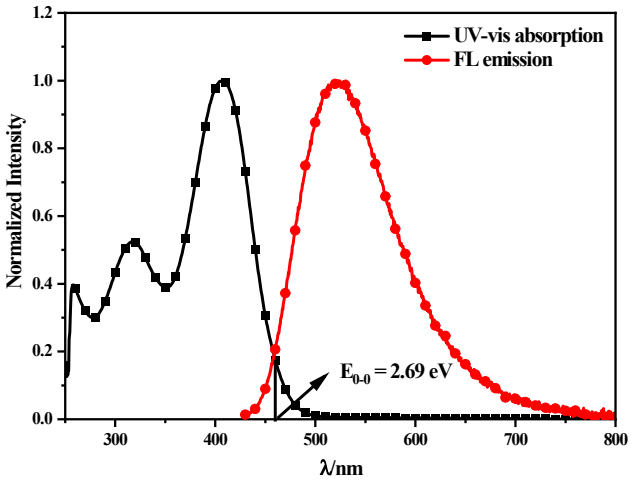

Figure S8. Normalized absorption and fluorescence emission spectra of MOC-Q3 in DMSO.

Table S7. H_2 production data of g-C_3N_4/MOC-Q3 (7/9/11/13 wt%) in 5 h.

Catalyst	H_2 production rate / mmol g^{-1} h^{-1}	H_2 production (5 h) / mmol g^{-1}	$TON_{[Pd]}$	$TON_{[MOC-Q3]}$
g-C_3N_4/MOC-Q3 (7 wt%)	30.3	151.5	69,834	209,502
g-C_3N_4/MOC-Q3 (9 wt%)	41.1	205.5	73,773	221,320
g-C_3N_4/MOC-Q3 (11 wt%)	50.1	250.5	76,889	230,667
g-C_3N_4/MOC-Q3 (13 wt%)	46.3	231.5	58,165	174,494
$Me_4(en)Pd(NO_3)_2$/g-C_3N_4/L-2 (11 wt%)	14.1	70.5	21,639	——
MOC-Q3	0.084	0.42	0.42	1.25

Table S8. Summarized literature data of photocatalytic water splitting by C_3N_4-based Z-scheme systems.

Entry	Catalysts	Electron mediator	Mass of catalyst (mg)	Reactant solution	Cocatalyst	Light source	H_2 and O_2 evolution rate / μmol h^{-1} g^{-1}	AQY	Reference
1	C_3N_4/C-TiO_2	Au	10	10 vol% TEOA aq.	——	300 W Xe lamp (>420 nm)	129 and –	——	*ChemCatChem* **2017**, 9, 3752-3761
2	C_3N_4/MoO_3	1T-MoS_2	10	10 vol% TEOA aq.	3 wt% Pt	300 W Xe lamp (>420 nm)	513.0 and –	——	*Nanoscale* **2018**, 10, 9292-9303
3	C_3N_4/CdS	rGO	20	H_2O/lactic acid v/v = 9:1	——	350 W Xe lamp (IR and UV filters)	396 and –	36.5%	*Chem. Eng. J.* **2017**, 317, 913-924
4	C_3N_4/Fe_2O_3	rGO	40	H_2O	Pt	300 W Xe lamp (>300 nm)	1,090 and 530		*Angew. Chem. Int. Ed.* **2019**, 58, 7102-7106
5	C_3N_4/MOFs	Aromatic rings	20	10 vol% TEOA aq.	3 wt% Pt	300 W Xe lamp (320-780 nm)	1123 and –	——	*Appl. Catal. B* **2018**, 220, 607-614
6	$Cd_xZn_{1-x}S$/g-C_3N_4	Au	50	0.1 M glucose aq.	——	300 W Xe lamp (>420 nm)	123.21 and –	——	*Sci. Bull.* **2017**, 62, 602-609
7	$Cd_{0.5}Zn_{0.5}S$/g-C_3N_4	RGO	30	0.35 M Na_2S/0.25 M Na_2SO_3 aq.	——	300 W Xe lamp	23,470 and –	37.88% at 420 nm	*Appl. Surf. Sci.* **2018**, 447, 783-794

8	Ag_3PO_4/g-C_3N_4	Ag and graphene	300	$AgNO_3$ aq. 10 g/L	——	30 W LED	– and 122	——	*Appl. Surf. Sci.* **2018**, 430, 108-115
9	Ag_3PO_4/g-C_3N_4	graphdiyne	200	H_2O	——	300 W Xe lamp (>420 nm)	– and 753.1	——	*Carbon* **2018**, 132, 598-605
10	Ag_3PO_4/g-C_3N_4	Ag	300	$AgNO_3$ aq. 10 g/L	——	White light LED	– and 110.1	——	*Appl. Surf. Sci.* **2018**, 430, 301-308
11	C_3N_4/Ag_3PO_4/Ag_2MoO_4	Ag	50	$AgNO_3$ aq. 10 g/L	——	30 W white LED	– and 924.6	——	*Appl. Surf. Sci.* **2018**, 456, 369-378
12	g-C_3N_4/MoS_2/Ag_3PO_4	MoS_2	300	$AgNO_3$ aq. 10 g/L	——	White light LED	– and 232	——	*Appl. Surf. Sci.* **2019**, 463, 9-17
13	C_3N_4/TiO2	None	50	10 vol% TEOA aq.	——	350 W Xe lamp	4128 and –	——	*Carbon* 2019, **149**, 618-626
14	C_3N_4/OD-ZnO	None	100	10 vol% TEOA aq	1 wt% Pt	300 W Xe lamp (>420 nm)	322 and –	——	*Appl. Catal. B* **2017**, 206, 406-416
15	C_3N_4/WO_3	None	50	10 vol% TEOA aq.	1 wt% Pt	300 W Xe lamp	3,120 and –	——	*Appl. Catal. B* **2017**, 219, 693-704
16	C_3N_4/$W_{18}O_{49}$	None	50	10 vol% TEOA aq.	3 wt% Pt	300 W Xe lamp (>420 nm)	8597 and –	39.1% at 420 nm	*Nano Energy* **2017**, 40, 308-316
17	C_3N_4/α-Fe_2O_3	None	100	25 vol% TEOA aq.	5 vol% Pt	300 W Xe lamp (>400 nm)	776 and –	——	*Int. J. Hydrogen Energy* **2017**, 42, 28327-28336
18	C_3N_4/α-Fe_2O_3	None	50	15 vol% TEOA aq.	1 wt% Pt	350 W Xe lamp (>420 nm)	398 and –	——	*Sol. RRL* **2018**, 2, 1800006
19	C_3N_4/MnO_2	None	10	10 vol% TEOA aq.	3 wt% Pt	300 W Xe lamp (>400 nm)	28000 and –	23.33% at 420 nm	*Appl. Catal., B* **2019**, 241, 452-460
20	C_3N_4/CdS	None	20 25	H_2O Na_2S (0.05	1 wt% Pt	300 W Xe lamp (>420 nm)	60.6 and 28.9 2,276 and –	—— 10.3% at 420	*ACS Catal.* **2018**, 8, 2209-2217

				M) and Na_2SO3 (0.1 M) aq.				nm	
21	C_3N_4/PTCDA	None	100	0.1 M $AgNO_3$ aq.	Co_3O_4	300 W Xe lamp (>420 nm)	- and 847	4.5% at 420 nm	*Appl. Catal. B* **2020**, 260, 118179
22	g-C_3N_4/WO_3	None	50	10 vol% TEOA aq.	1 wt% Pt	300 W Xe lamp (>420 nm)	400 and –	——	*Nanotechnology* **2017**, 28, 164002
23	WO_3/g-C_3N_4	None	50	15 vol% TEOA aq.	$Ni(OH)_x$	300 W Xe lamp (>400 nm)	576 and –	——	*Chin. J. Catal.* **2017**, 38, 240-252
24	g-C_3N_4/WO3	None	50	20 vol % lactic acid aq.	2 wt% Pt	350 W Xe lamp (full spectrum)	982 and –	——	*Appl. Catal. B* **2019**, 243, 556-565
25	g-C_3N_4/TiO_2	None	100	10 vol% TEOA aq.	0.1 M Pt	300 W Xe lamp (>400 nm)	1938 and –	——	*Appl. Surf. Sci.* **2018**, 448, 288-296
26	MoS_2/g-C_3N_4	None	50	25 vol% methanol aq.	2 wt% Pt	300 W Xe lamp (>420 nm)	577 and –	——	*Appl. Catal. B* **2018**, 228, 64-74
27	$CuInS_2$/g-C_3N_4	None	50	10 vol% TEOA, 0.25 M Na_2S, and 0.2 M Na_2SO_3 aq.	——	300 W Xe lamp (>420 nm)	1,290 and –	——	*ACS Appl. Mater. Interfaces* **2017**, 9, 24577-24583
28	g-C_3N_4/Ag_2CrO_4	None	50	75mL water and 25mL	0.6 wt% Pt	300 W Xe lamp (>420 nm)	902.1 and –	——	*Sci. Rep.* **2018**, 8, 16504

				methanol (with 10 mM $NaHCO_3$)					
29	g-C_3N_4/PSi	None	100	10 vol% TEOA aq.	3 wt% Pt	300 W Xe lamp (400 nm)	870.5 and –	——	*J. Catal.* **2017**, 356, 22-31
30	g-C_3N_4/SiC	None	50	10 vol% TEOA aq.	1 wt% Pt	300 W Xe lamp (>420 nm)	182 and –	——	*Appl. Surf. Sci.* **2017**, 391, 449-456
31	$MnIn_2S_4$/g-C_3N_4	None	50	0.35 M Na_2S/0.25 M Na_2SO_3 aq.	——	300 W Xe lamp (>400 nm)	208 and —	——	*Chem. Eng. J.* **2019**, 359, 244-253
32	ZnO/ZnS/g-C_3N_4	None	100	0.25 M Na_2S/0.25 M Na_2SO_3 aq.	——	300 W Xe lamp	301.25 and –	——	*Appl. Surf. Sci.* **2018**, 430, 293-300
33	Ag_3PO_4/g-C_3N_4	None	300	H_2O	1 g $AgNO_3$	25 W LED	– and 228.8	——	*Appl. Catal. B* **2019**, 244, 240-249
34	Ag_3PO_4/g-C_3N_4	None	40	0.02 M AgNO3 aq.	——	300 W Xe lamp (>420 nm)	– and 520	20.2% at 420 nm	*Mater. Lett.* **2017**, 201, 66-69
35	TiO_2/g-C_3N_4	None	100	10 vol% TEOA aq.	1 wt% Pt	150 W Xe lamp	1,540 and –	——	*Appl. Catal. B* **2016**, 191, 130-137
				NaI aq. (5 mM)	1 wt% Pt and1 wt% PtO_x		102.3 and 52.8	2.06% at 425 nm	
36	Zn-doped g-	None	100	H_2O	1 wt% Pt	300 W Xe lamp	2,100 and 1,050	——	*Chin. J. Catal.* **2018**, 39, 472-478

	$C_3N_4/BiVO_4$								
37	α-Fe_2O_3/g-C_3N_4	None	10	H_2O	3 wt% Pt	300 W Xe lamp (>400 nm)	31400 and –	44.35% at 420 nm	*Adv. Energy Mater.* **2017**, 7, 1700025
		None	50	10 vol% TEOA aq.	3 wt% RuO_2	300 W Xe lamp (>400 nm)	38.2 and 19.1	——	
38	S-g-$C_3N_4/WO_{2.72}$	None	50	9 vol% TEOA aq.	——	300 W Xe lamp (>420 nm)	786 and –	7.6% at 420 nm	*Nano Energy* **2021**, 81, 105671
39	Py-g-C_3N_4 tube	None	20	10 vol% TEOA aq.	1 wt % Pt	300 W Xe lamp (>420 nm)	4548.4 and –	2.16% at 420 nm	*Chem. Eng. J.* **2021**, 414, 128802
40	g-C_3N_4/NCDS	None	50	10 vol% TEOA aq.	MoS_2	300 W Xe lamp (>420 nm)	212.41 and –	——	*Appl. Catal. B* **2019**, 247, 124-132
41	$Ni(OH)_2$/g-C_3N_4	None	20	20 vol% TEOA aq.	——	300 W Xe lamp (>420 nm)	4,360 and –	8.2% at 400 nm	*Appl. Catal. B* **2019**, 258, 117997
42	3.8-MoCN	None	5	20 vol% TEOA aq.	1 wt % Pt	300 W Xe lamp (>400 nm)	1265 and –	1.64% at 400 nm	*Appl. Catal. B: Environ* **2023,** 336, 122907
43	M+U-3	None	50	10 vol% TEOA aq.	1 wt % Pt	300 W Xe lamp (>400 nm)	744 and –	21.6% at 400 nm	*Appl. Catal. B: Environ.* **2023,** *333*, 122805
44	CN-C	None	20	10 vol% TEOA aq.	3 wt% Pt	300 W Xe lamp (>420 nm)	468.8 and –	15.56% at 385 nm	*Chin. J. Catal.* **2023,** *50*, 361-371
45	CN/CNQDs-20–6 h	None	20	10 vol% TEOA aq.	2 wt% Pt	300 W Xe lamp (>420 nm)	3640.6 and –	6.74% at 420 nm	*Appl. Catal. B: Environ* **2023,** *339*, 123101
46	Pt-hCN/$Co(OH)_2$-B-hCN	None	50	H_2O	3 wt%Pt and 3 wt% $Co(OH)_2$	300 W Xe lamp (>320 nm)	1508 and 760	30.1% at 420 nm	*ACS Energy Lett.* **2024,** *9*, 1915-1922
47	HCN	None	50	10 vol% TEOA aq.	3 wt% Pt	300 W Xe lamp (>420 nm)	7840 and –	24.1% at 420 nm	*Appl. Catal. B: Environ.* **2024,** *350*, 123902.

48	$B_{1.0}CR_{0.5}PCN$	None	20	H_2O	1 wt % Pt	300 W Xe lamp (>420 nm)	615 and 310	2.11% at 420 nm	*Chem. Eng. J.* **2023,** *470*, 144199
49	PCN-$SrTiO_3$	None	50	H_2O	3 wt%Pt and CoOx	300 W Xe lamp (>300 nm)	202 and 118	——	*Chin. J. Catal.* **2023,** *48*, 279-289
50	CoP/CoO@g-C_3N_4	None	50	H_2O	CoP and CoO	300 W Xe lamp (>420 nm)	133.2 and 67.2	0.92% at 360 nm	*Appl. Catal. B: Environ.* **2024**, 124527
51	MOC-Q3/g-C_3N_4	None	5	10 vol% TEOA aq.	——	300 W Xe lamp (>420 nm)	50,100 and –	31.6% at 425 nm	This work
			10	H_2O			77.32 and 38.06		

Table S9. AQY(%) values of g-C_3N_4/MOC-Q3 (7/9/11/13 wt%) at different wavelengths.

Sample	AQY at 425 nm / %	AQY at 450 nm / %	AQY at 515 nm / %
g-C_3N_4/MOC-Q3 (7 wt%)	16.5	9.40	0.05
g-C_3N_4/MOC-Q3 (9 wt%)	21.9	10.3	0.07
g-C_3N_4/MOC-Q3 (11 wt%)	31.6	17.3	0.10
g-C_3N_4/MOC-Q3 (13 wt%)	23.5	12.2	0.08

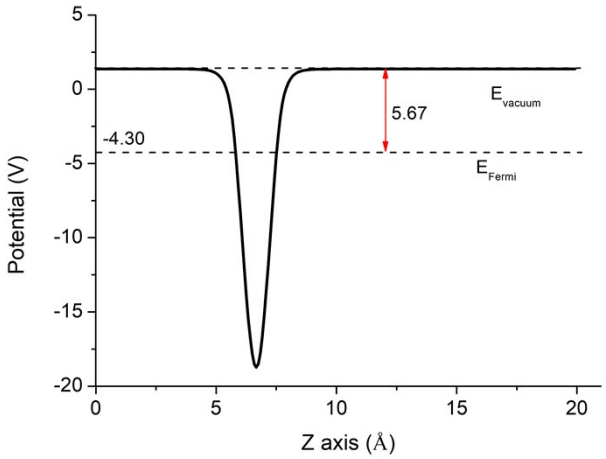

Figure S9. Local potential of g-C_3N_4.

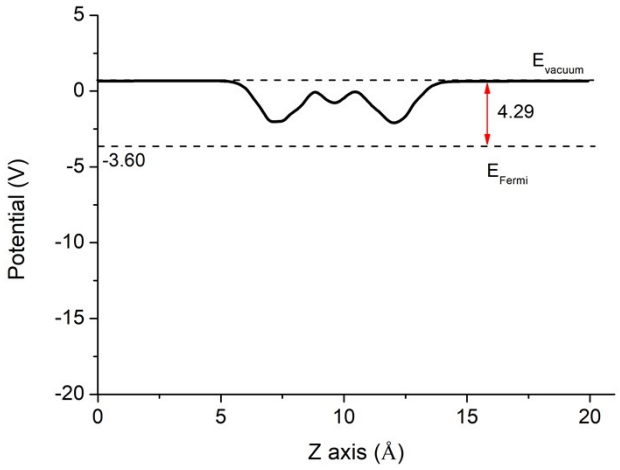

Figure S10. local potential of MOC-Q3.

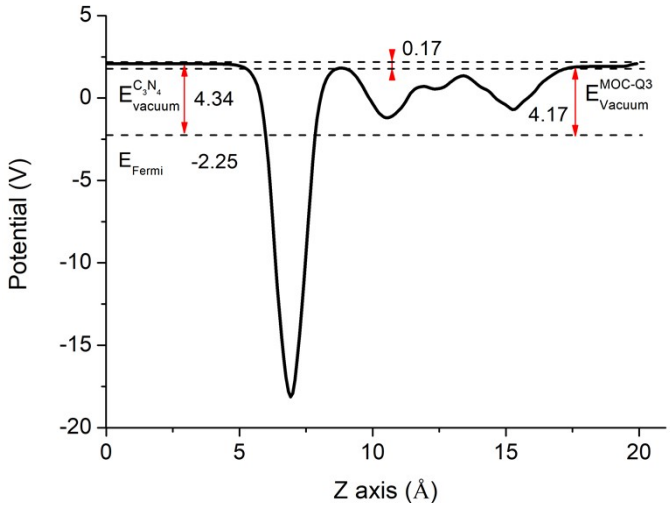

Figure S11. Local potential of g-C_3N_4/MOC-Q3 model.

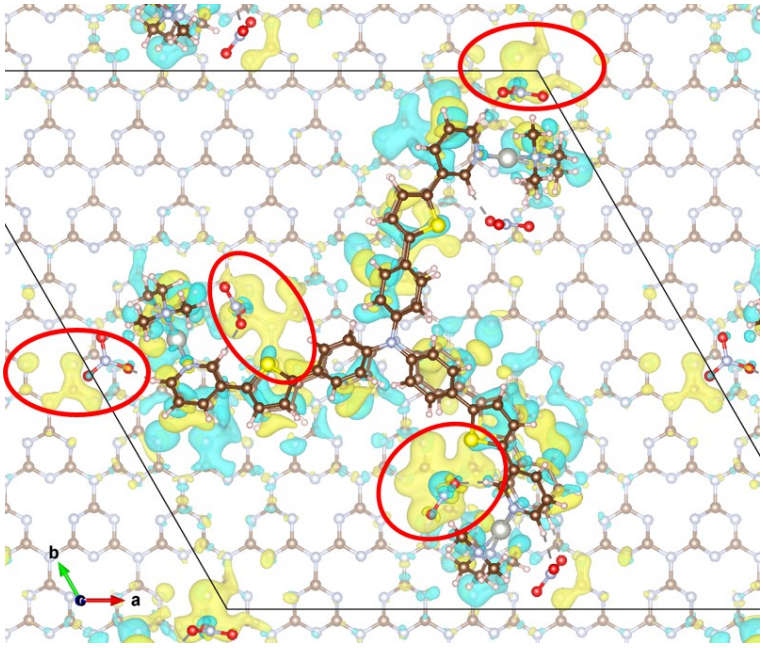

Figure S12. Charge transfer between g-C_3N_4/MOC-Q3 model. Yellow region lose electron; cyan region obtain electron. Red frames show charge loss of g-C_3N_4 due to NO_3^- groups.

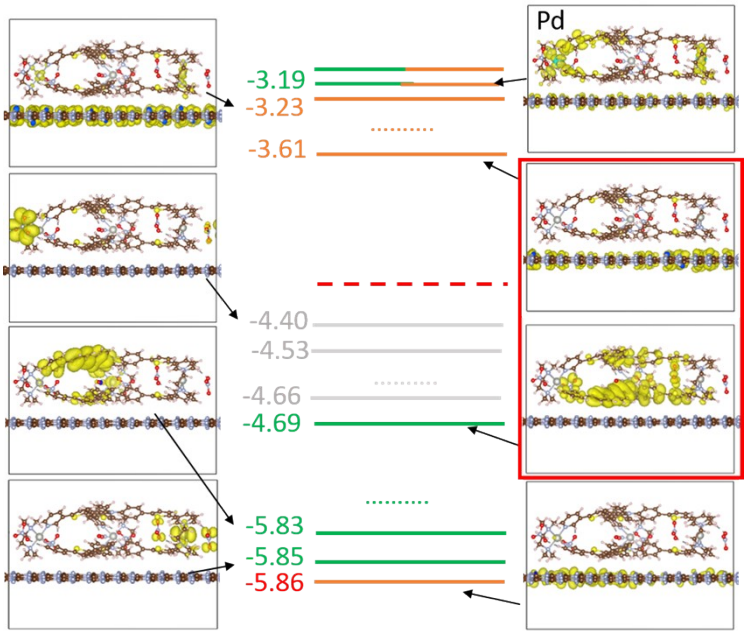

Figure S13. Energy levels near Fermi level and their corresponding orbitals of the g-C_3N_4/MOC-Q3 model.

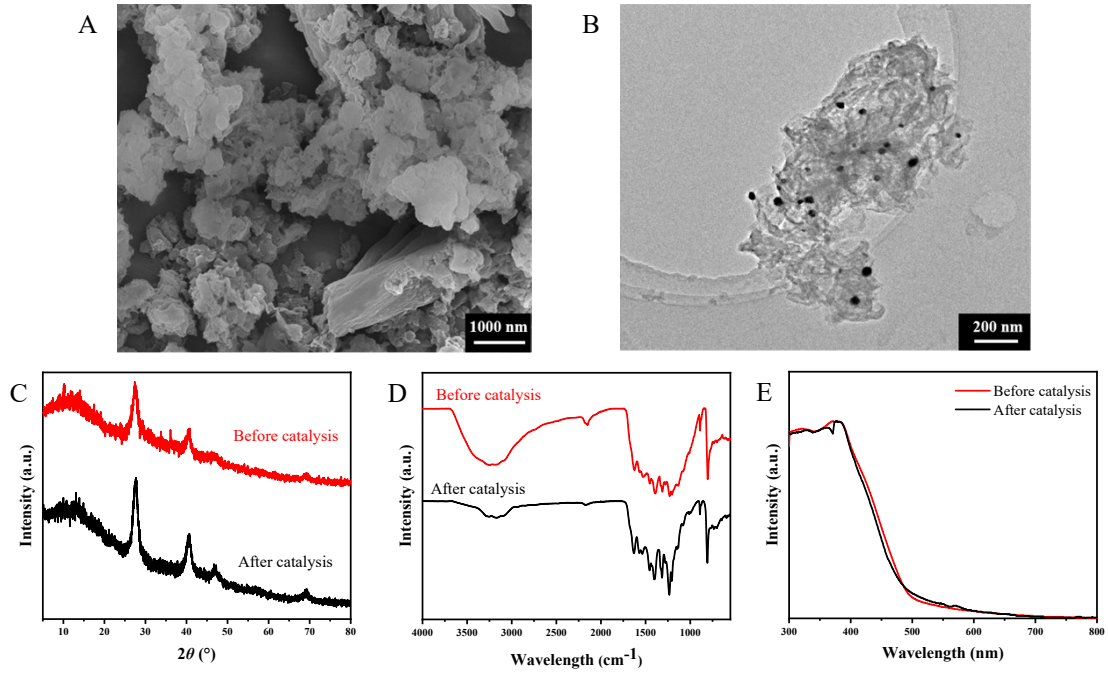

Figure S14. A) SEM and B) TEM images of IrO_2/g-C_3N_4/MOC-Q3, C) PXRD, D) FT-IR spectroscopy, and E) UV-Vis solid absorption spectroscopy of IrO_2/g-C_3N_4/MOC-Q3 before and after long-term reaction.

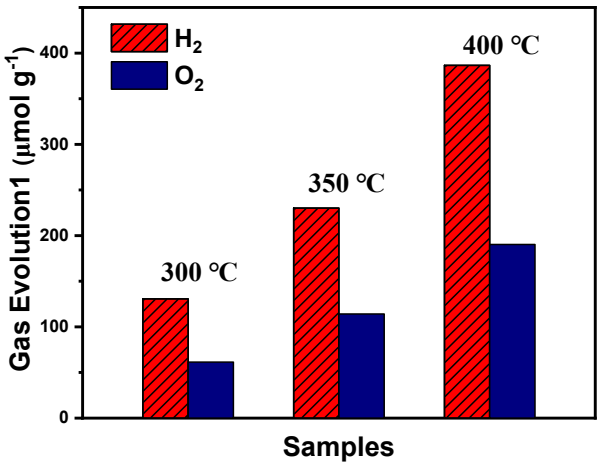

Figure S15. The H_2 and O_2 production performances of IrO_2/g-C_3N_4/MOC-Q3 composites prepared at different calcination temperatures.

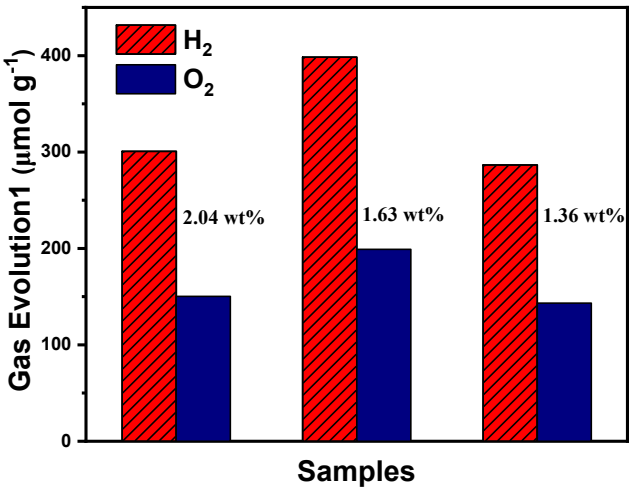

Figure S16. The H_2 and O_2 production performances of IrO_2 (2.04/1.63/1.36 wt%)/g-C_3N_4/MOC-Q3 composites.

Reference

1. T.-T. Bui, L. Beouch, X. Sallenave, F. Goubard, Carbazol-N-yl and Diphenylamino End-Capped Triphenylamine-based Molecular Glasses: Synthesis, Thermal, and Optical Properties. *Tetrahedron Lett.* **2013**, *54*, 4277-4280. DOI: 10.1016/j.tetlet.2013.05.152